Journal of the European Ceramic Society 16 (1996) 1201-1207

0955-2219/96/$15.00
PII:S0955-2219(96)00055-6

Discrimination of Multiaxiality Criteria Using Brittle Fracture Loci

A. Brückner-Foit,[a] T. Fett,[b] K.-S. Schirmer[a] & D. Munz[a]

[a]Karlsruhe University, Institute for Reliability and Failure Analysis, PO Box 36 40, D-76021 Karlsruhe, Germany
[b]Research Centre, Karlsruhe, IMF II, PO Box 36 40, D-76021 Karlsruhe, Germany

(Received 19 December 1995; revised version received 26 February 1996; accepted 28 February 1996)

Abstract

The statistical distribution of brittle fracture loci was measured in the Brazilian disc test. A logical circuit was used to identify the fracture event in addition to fractographic examination. The empirical distribution of brittle fracture loci is compared with the predictions of the multiaxial Weibull theory. The results indicate that a shear-insensitive criterion is more suitable than a shear-sensitive criterion to describe the fracture behaviour of natural flaws in ceramic materials. Copyright © 1996 Elsevier Science Ltd

1 Introduction

The failure behaviour of ceramics under multiaxial loading can be described by the Weibull theory, which is developed in Refs 1–4. In this theory, the failure behaviour of natural flaws such as pores, inclusions and grain boundary wedges, is analysed by a fracture mechanics model. The natural flaws are replaced by planar cracks of ideal shapes, and the loading of each crack is quantified in terms of the corresponding stress intensity factors. In general, a randomly oriented crack in a multiaxial stress field is subjected to mixed-mode loading, and an appropriate multiaxiality criterion has to be chosen (see Ref. 5 for a summarizing description of available criteria).

Keeping in mind that the planar cracks in the Weibull theory are in reality natural flaws of various shapes and differing in physical nature, it cannot be concluded without a substantial amount of experimental evidence that there is a universal multiaxiality criterion.[6] Rather, the multiaxiality criterion seems to be specific to a given material and has to be determined by suitable experimental procedures.

Ceramic components are designed to meet a given level of reliability. Within the framework of the Weibull theory, the calculated value of reliability depends on the Weibull parameters and on the multiaxiality criterion. While there is a standard procedure for estimating the Weibull parameters (e.g. Ref. 7), no commonly accepted method exists for determining the failure behaviour of ceramics under multiaxial loading. It can be shown[5] that the variation of the calculated reliability value with the multiaxiality criterion is almost negligible compared with the accuracy of the experimental results if failure is triggered from regions in which a stress state with positive principal stresses prevails. However, great differences may occur if there are positive and negative principal stresses in critical regions, e.g. if a uniaxial tensile operational stress is superimposed on compressive residual stresses. Hence, the multiaxiality criterion can be determined by comparing two different test series — the first performed with specimens in which a tensile stress state prevails, and the second performed with specimens in which the stress tensor is composed of positive and negative principal stresses. Examples are given in Refs 8 and 9.

The problem with all these test series is that specimens having different shapes that were made using different finishing and possibly manufacturing procedures have to be compared with each other. This may lead to incompatible results,[8] even though the Weibull theory is still valid. Hence, a test procedure relying on only one type of specimen seems to be necessary.

This paper deals with the theoretical and experimental evaluation of the local risk of rupture,[10,11] which can be used to discriminate between multiaxiality criteria. The following section contains the definition of the local risk of rupture and the corresponding cumulative distribution function. This quantity can be determined if the location of the critical flaw is measured on the fracture surface of a failed specimen. The corresponding experimental procedure is described in the next section. The experimental results including the Weibull analysis are then presented, while theory and experiment are compared in the final section.

Theory

Most of the information presented in this section has already been given in previous publications[5,11] and is repeated here for the sake of completeness. First, the basic ideas of the Weibull theory will be summarized. The probability that the size of a given flaw will exceed the critical flaw size a_c is expressed by:

$$Q_1 = \int_V f_x(x) \int_\Omega f_\Omega(\Omega) \int_{a_c(x,\Omega)}^{\infty} f_a(a)\, da\, d\Omega\, dx \quad (1)$$

where V denotes the volume of the component considered, Ω the surface of a unit radius sphere, x the coordinate vector, and $f_x(x)$, $f_\Omega(\Omega)$, $f_a(a)$ are the probability density functions of the corresponding random variables.

The critical flaw size can be determined using fracture mechanics, if the natural flaws can be approximated by planar cracks. Within the framework of this model, a multiaxial stress state gives rise to mixed-mode loading of a crack, and the critical crack size is a function of the mode I to mode III stress intensity factors K_I, K_{II}, K_{III}:

$$a_c = a_c(K_I, K_{II}, K_{III}) \quad (2)$$

with

$$\begin{aligned} K_I &= \sigma_n \sqrt{a Y_I} \\ K_{II} &= \tau \sqrt{a Y_{II}} \\ K_{III} &= \tau \sqrt{a Y_{III}} \end{aligned} \quad (3)$$

where Y_I, Y_{II} and Y_{III} are correction factors. The stress σ_n normal to the crack plane is given by the following relation:

$$\sigma_n = (\sigma_1 \cos^2\phi + \sigma_2 \sin^2\phi)\sin^2\theta + \sigma_3 \cos^2\theta \quad (4)$$

where σ_1, σ_2, σ_3 are the principal stresses and ϕ, θ are the polar angles determining the orientation of the crack plane relative to the principal axes. The shear stress τ in the crack plane is given by:

$$\tau = \sqrt{\tau_{r\phi}^2 + \tau_{r\theta}^2} \quad (5)$$

with

$$\tau_{r\phi} = (\sigma_2 - \sigma_1)\sin\phi \cos\phi \sin\theta \quad (6)$$

and

$$\tau_{r\theta} = (\sigma_1 \cos^2\phi + \sigma_2 \sin^2\phi - \sigma_3)\sin\theta\cos\theta \quad (7)$$

An equivalent mode I stress intensity factor K_{Ieq} can be introduced with

$$K_{Ieq} = \sigma_{eq}\sqrt{a Y_I} \quad (8)$$

where the equivalent stress σ_{eq} depends on σ_n, τ and on Y_I, Y_{II} and Y_{III}. The critical crack size is given by:

$$a_c = \left(\frac{K_{Ic}}{\sigma_{eq} Y_I}\right)^2 \quad (9)$$

where K_{Ic} denotes the fracture toughness. A variety of multiaxiality criteria are given in the literature leading to different expressions for σ_{eq}. A summary is contained in Ref. 5.

An example of one of these criteria for penny-shaped cracks is[12]

$$\sigma_{eq} = \left[\sigma_n^4 + 6\left(\frac{2}{2-\nu}\right)^2 \sigma_n^2 \tau^2 + \left(\frac{2}{2-\nu}\right)^4 \tau^4\right]^{1/4} \quad (10)$$

which is derived on the assumption that the crack extends on the plane where the energy release rate is maximum. The shear insensitive criterion:

$$\sigma_{eq} = \sigma_n \quad (11)$$

is applicable if the natural flaws extend solely because of mode I loading.

In the Weibull theory the following expression is used for the integral over the crack size in eqn (1):[7]

$$\int_{a_c(x,\Omega)}^{\infty} f_a(a)da = \left(\frac{\sigma_{eq}(x,\Omega)}{\tau_0}\right)^m \quad (12)$$

where eqn (9) was used for the critical crack size. The parameters m and τ_0 in eqn (12) depend on the toughness of the matrix material and on the statistical properties of the flaw size distribution.

If all locations of flaws and all orientations occur with equal probability, the material is homogeneous and isotropic, and $f_x(x)$ and $f_\Omega(\Omega)$ can be replaced by uniform distributions:

$$Q_1 = \frac{1}{V}\int_V \frac{1}{4\pi}\int_\Omega \left(\frac{\sigma_{eq}}{\tau_0}\right)^m d\Omega dx \quad (13)$$

The number n of cracks in the volume V is also a random variable and can be described by a Poisson distribution. The probability of having exactly n cracks in V is given by:

$$p_n = \frac{M^n e^{-M}}{n!} \quad (14)$$

where M is the average number of cracks in V. The following relation is obtained for the failure probability P_f, from eqns (13), (14)[5] and by summing up all possible numbers of cracks:

$$P_f = 1 - \exp(-M Q_1) \quad (15)$$

These basic ideas of the Weibull theory will now be used to define the local risk of rupture.

The probability that a flaw is located in a subvolume V_s and propagates unstably is equal to

$$Q_1(V_s) = \frac{1}{V}\int_{V_s} \frac{1}{4\pi}\int_\Omega \left(\frac{\sigma_{eq}}{\tau_0}\right)^m d\Omega dx \quad (16)$$

The survival probability of a flaw located in V_s or $V - V_s$ is given by:

$$R_1(V) = 1 - Q_1(V) \tag{17}$$

If n flaws are present in V, none of them propagates unstably with the probability

$$R_n(V) = (1 - Q_1(V))^n \tag{18}$$

Hence fracture is triggered by one flaw in V_s and all other $n - 1$ flaws remain stable with the probability

$$S_n(V_s) = n\, Q_1(V_s)\,(1 - Q_1(V))^{n-1} \tag{19}$$

Combining eqn (19) with the probability p_n, eqn (14), to have n flaws in V and summation over n yields the probability that there is exactly one unstable flaw contained in the subvolume V_s and an arbitrary number of non-propagating flaws in V:

$$S(V_s) = \sum_{n=0}^{\infty} p_n\, S_n(V_s) \tag{20}$$

i.e.

$$S(V_s) = M\, Q_1(V_s) \exp(-M\, Q_1(V)) \tag{21}$$

The normalized quantity

$$P_0(V_s) = \frac{S(V_s)}{S(V)} \tag{22}$$

is the quotient of the fracture risks associated with the volumes V_s and V, respectively, and can be written as:

$$P_0(V_s) = \frac{Q_I(V_s)}{Q_I(V)} \tag{23}$$

$P_0(V_s)$ is independent of the applied load level.

For a very small subvolume, $V_s = \mathrm{d}x$, the integral over V_s can be replaced by the integrand times dx, and the probability is obtained that failure is caused by a flaw at point x in the interval $[x, x + \mathrm{d}x]$:

$$p_0(x)\,\mathrm{d}x = \frac{\int_\Omega (\sigma_{eq})^m\, \mathrm{d}\Omega}{\int_V \int_\Omega (\sigma_{eq})^m\, \mathrm{d}\Omega \mathrm{d}x} \tag{24}$$

The quantity p_0 corresponds to the marginal probability density function of the location of the fracture origins obtained by Matsuo and Kitakami[10] using the competing risk theory, and P_0 in eqn (23) is the corresponding probability distribution function if V_s is defined as an interval in three-dimensional space. p_0 also corresponds to the local risk of fracture.

The cumulative probability distribution function of the fracture loci:

$$P_0(X \le x_0,\ Y \le y_0,\ Z \le z_0)$$

$$= \frac{\int_0^{x_0} \int_0^{y_0} \int_0^{z_0} \int_\Omega \sigma_{eq}^m(\Omega, x, y, z)\, \mathrm{d}\Omega\, \mathrm{d}z\mathrm{d}y\mathrm{d}x}{\int \int_V \int \int_\Omega \sigma_{eq}^m(\Omega, x, y, z)\, \mathrm{d}\Omega\, \mathrm{d}z\mathrm{d}y\mathrm{d}x} \tag{25}$$

can be determined for any specimen or component, if the location (x_0, y_0, z_0) of the fatal flaw is measured.

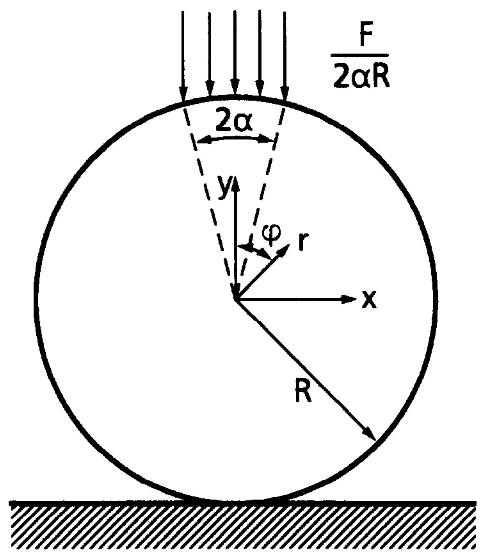

Fig. 1. Brazilian disc test.

Experiments

In the Brazilian disc test a circular disc is subjected to diametral compression (Fig. 1). A biaxial stress state is induced which contains both tensile and compressive components (see next section). The test was applied successfully to rock materials and low-strength ceramics.[13,14] Preliminary tests with high-strength ceramics[15] showed that fracture of the majority of specimens was triggered by flaws on the perimeter in the vicinity of the load pins where a zone of global damage develops due to high compressive loads. An additional failure mode (splitting of a specimen parallel to the disc surface) could be attributed to high tensile stresses on the perimeter normal to the disc surface that are induced by friction between the load pins and the disc.[16] These unwanted failure modes can be almost completely eliminated by a special design of the specimen grips (Fig. 2). A compressive force perpendicular to the disc surface is imposed by the screws in the vicinity of the load pins.

The location of the fracture origins was measured in two different ways. First, a careful fractographic examination was carried out in which both the fracture pattern (see Fig. 3) and the fracture surfaces were studied. In a second method of evaluation, a series of parallel conducting strips of silver was deposited on the disc surfaces. They were used as logical electrical switches which are in the 'on' state in the case of the intact disc and change to the 'off' state upon passage of the crack tip. A logical circuit analyses the time sequence of rupture and allows the location of the failure origin to be determined.

A mounted specimen is shown in Fig. 4. The fracture origin is assumed to be located in the vicinity of the first ruptured strip. Those specimens for which no fracture locus could be identified

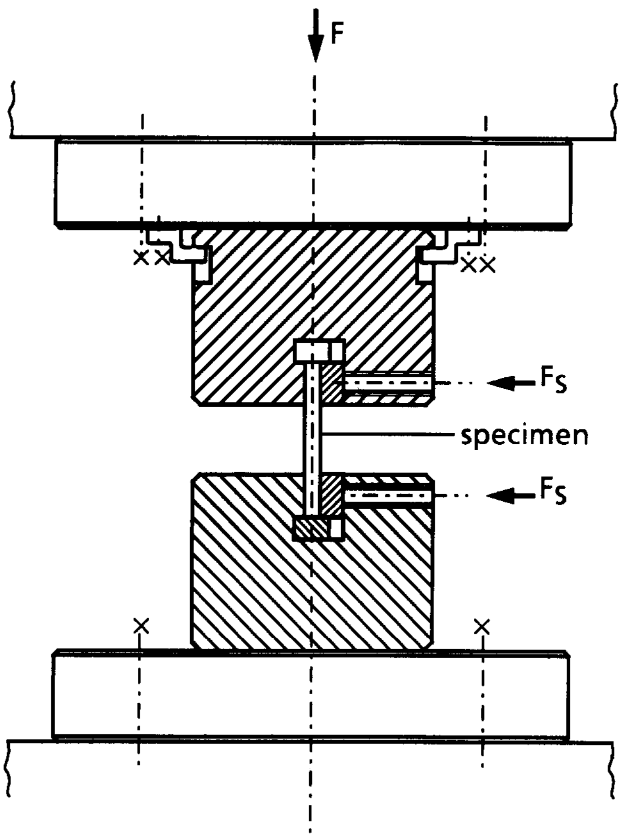

Fig. 2. Schematic representation of the test rig for the Brazilian disc test.

outside the specimen grips were eliminated from the test series, because failure may have been triggered from the damage zone in the vicinity of the load pins.

Three different materials were tested, a low-strength ceramic (stoneware trade name: Keraion), and two high-strength silicon nitride materials. The material parameters are summarized in Table 1. The radius of the discs was $R = 22{\cdot}5$ mm in all cases. The thickness t of the stoneware disks was

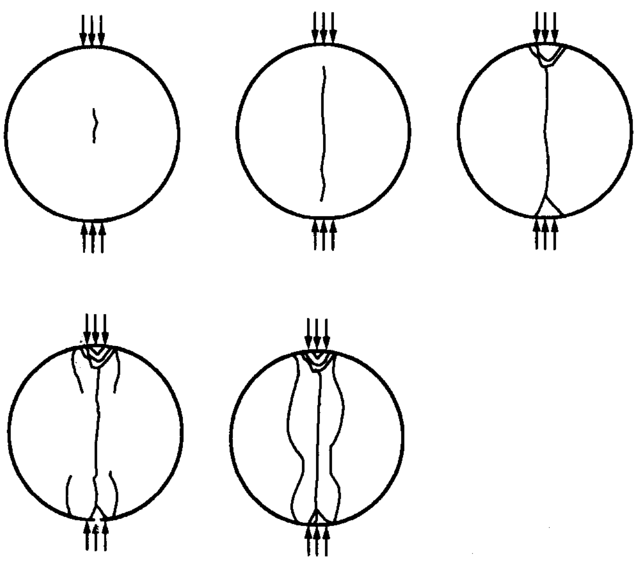

Fig. 3. Development of a typical fracture pattern starting from a central crack.

7·4 mm, whereas $t = 4{\cdot}0$ mm was used for the silicon nitrides. The loading rate was comparatively small (7 MPa s^{-1} for the stoneware material, 3 MPa s^{-1} for the silicon nitrides) in order to avoid complete specimen destruction after fracture. The load was transferred to the disc via comparatively soft steel plates, which deformed plastically under the high compressive loads.

Results

The Weibull exponent m is required for the prediction of the distribution of fracture loci [see eqn (24)]. Therefore, a statistical analysis was performed of the fracture stresses. First, the test results were plotted on Weibull paper. Then, the parameters of the corresponding Weibull distributions were calculated using the maximum likelihood method.[17] A bias correction factor was introduced for the parameter m.[17] The results of the Weibull analysis are summarized in Table 2. The Weibull parameter b in Table 2 is defined as:

$$b = \tau_0 \left[\frac{M}{V}\int_V \frac{1}{4\pi}\int_\Omega \left(\frac{\sigma_{eq}}{\sigma^*}\right)^m \mathrm{d}\Omega \mathrm{d}x\right]^{-1/m} \quad (26)$$

with the reference stress σ^*, from which the failure probability can be written in terms of a Weibull distribution:

$$P_f = 1 - \exp\left[-\left(\frac{\sigma^*}{b}\right)^m\right] \quad (27)$$

The fractographic examination yielded results which are only reliable for the silicon nitrides. The fracture loci were very hard to identify on the fracture surface for the stoneware material, and the analysis had to be based on the rupture of the silver strips. Hence, only the y-coordinate of the fracture loci (see Fig. 1) was available.

The observed values y_i were ranked in ascending order and the empirical probability

$$P_i\,(y_i) = \frac{i}{N} \quad (28)$$

was attributed to the ith value, where N is the sample size. The resulting step functions are shown in Figs 5–7.

Discussion

The stress field of the Brazilian disc is given by:[18]

$$\sigma_{rr} = -\frac{F}{\pi\, t\, R} \quad (29)$$

$$\times \left\{1 + \sum_{n=1}^{\infty}\left[1 - \left(1 - \frac{1}{n}\right)\frac{r^2}{R^2}\right]\left(\frac{r}{R}\right)^{2n-2} \frac{\sin 2n\alpha}{\alpha} \cos 2n\phi\right\}$$

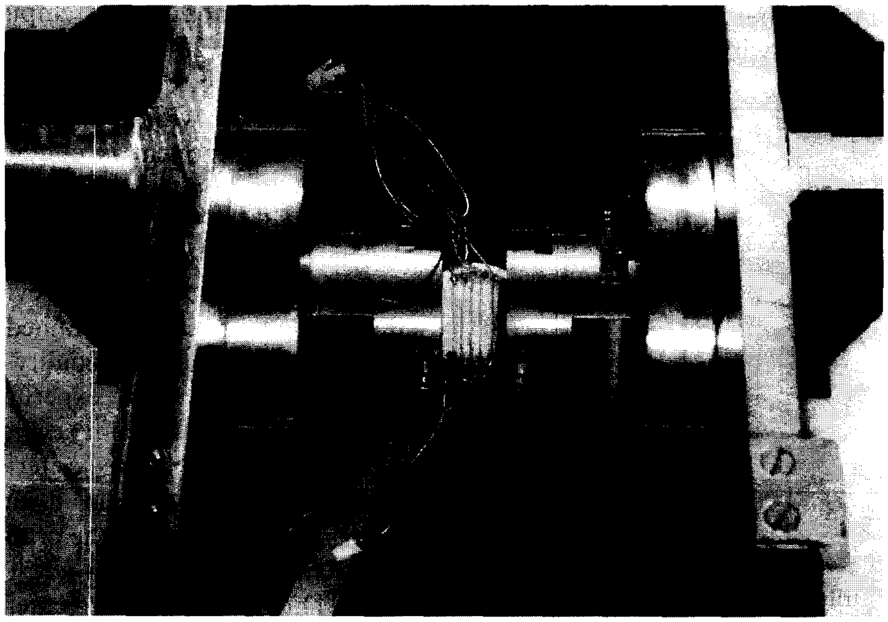

Fig. 4. Fixture with specimen mounted.

$$\sigma_{\phi\phi} = -\frac{F}{\pi\, t\, R} \tag{30}$$
$$\times \left\{1 - \sum_{n=1}^{\infty}\left[1-\left(1+\frac{1}{n}\right)\frac{r^2}{R^2}\right]\left(\frac{r}{R}\right)^{2n-2}\frac{\sin 2n\alpha}{\alpha}\cos 2n\phi\right\}$$

$$\sigma_{r\phi} = -\frac{F}{\pi\, t\, R} \tag{31}$$
$$\times \left\{\sum_{n=1}^{\infty}\left[1-\left(1+\frac{1}{n}\right)\frac{r^2}{R^2}\right]\left(\frac{r}{R}\right)^{2n-2}\frac{\sin 2n\alpha}{\alpha}\cos 2n\phi\right\}$$

where r, ϕ are the polar coordinates defined in Fig. 1. The loading angle α defines the area on the perimeter over which the load is uniformly distributed. The stress fields perpendicular to the loading axis ($y = 0$) and along the loading axis ($x = 0$) are shown in Figs 8 and 9, respectively.

This stress field is inserted in the appropriate multiaxiality criterion, eqns (10) and (11), respectively, in order to determine σ_{eq} which, in turn, is inserted in the marginal probability distribution of fracture loci:

$$P_0\,(Y \le y_0) = \frac{2\int_0^{\pi}\int_0^{r_0}\int_0^{t}\int_{\Omega}\sigma_{eq}^{m}\,d\Omega\,dz\,r\,dr\,d\phi}{2\int_0^{\pi}\int_0^{R}\int_0^{t}\int_{\Omega}\sigma_{eq}^{m}\,d\Omega\,dz\,r\,dr\,d\phi} \tag{32}$$

where $y_0 = r_0 \sin\phi$ and r and ϕ are the polar coordinates defined in Fig. 1; R denotes the radius of the disc, and t its thickness.

Table 1. Material parameters

Material	*Manufacturer*	*Poisson's ratio*	*Young's modulus (GPa)*	*Fracture toughness ($MPa\sqrt{m}$)*
Keraion (stoneware)	Keramische Betriebe Buchtal	0·25	52	0·9
HIPSN	ABB	0·24	300	4·3
HIPSN	ESK	0·24	300	4·9

Table 2. Results of Weibull analysis

Material	*Sample size*	*Weibull exponent,* m	*Weibull parameter,* b *(MPa)*
Stoneware	20	35·6 [26·4, 48·4]	37·5 [37·1, 37·9]
HIPSN (ABB)	14	10·5 17·3. 15·2]	553 [529, 579]
HIPSN (ESK)	21	6·0 [4·5, 8·2]	672 [630, 718]

Equation (32) implies that fracture is triggered from a flaw at $0 \le y \le y_0$ with the probability P_0.

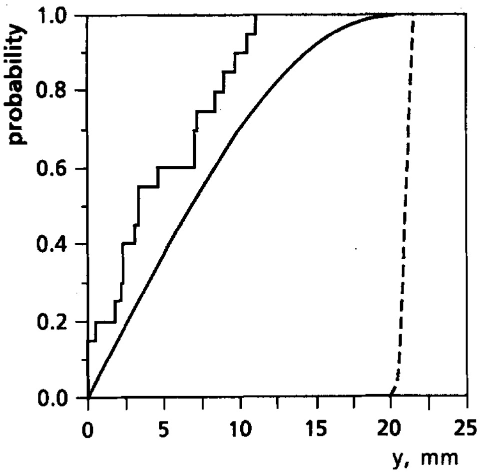

Fig. 5. Cumulative distribution function of brittle fracture loci, stoneware material: ———, prediction using the shear-insensitive criterion, eqn (11); – – – –, prediction using the shear-sensitive criterion, eqn (10).

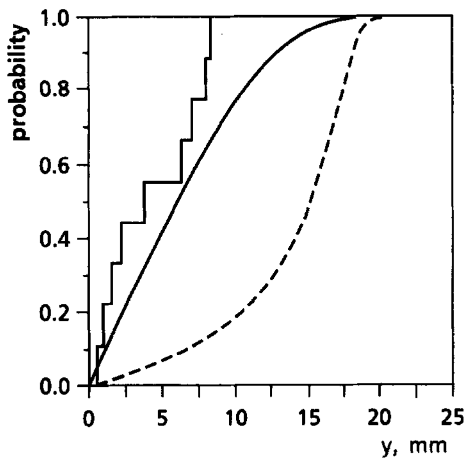

Fig. 6. Cumulative distribution function of brittle fracture loci, HIPSN (ABB material); ———, prediction using the shear-insensitive criterion, eqn (11); – – – –, prediction using the shear-sensitive criterion, eqn (10).

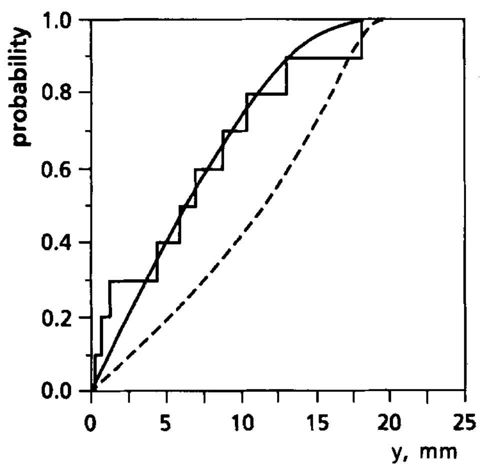

Fig. 7. Cumulative distribution function of brittle fracture loci, HIPSN (ESK material): ———, prediction using the shear-insensitive criterion, eqn (11); – – – –, prediction using the shear-sensitive criterion, eqn (10).

This corresponds to the empirical probability p_i defined in eqn (28). The integrals in eqn (32) were evaluated using the multiaxiality criteria [eqns (10) and (11)], with the bias-corrected values of the Weibull exponent m contained in Table 2. In Figs 5–7 the results are compared with the experimental findings.

The empirical distribution of the fracture loci of the stoneware material deviates strongly from the theoretical curve obtained with eqn (32) if a shear-sensitive multiaxiality criterion is used. The theoretical and experimental distribution functions are only compatible with each other if the shear-insensitive criterion is applied. In this case, the maximum distance between both curves does not exceed the critical distance defined in a Kolmogorov–Smirnov test at 95% confidence level. This result is in agreement with the findings in Ref. 9 where the distributions of fracture stress obtained in different test series including the Brazilian disc test were compared with each other.

Similar results are obtained for the silicon-nitride materials. The difference between the shear-sensitive and the shear-insensitive criteria is less pronounced than for the Keraion material due to lower values of the Weibull exponent m. Nevertheless, the shear-sensitive criterion is ruled out by comparison of the theory with the experiment,

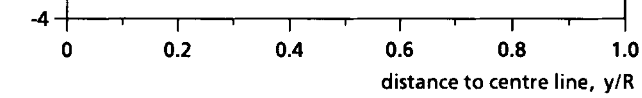

Fig. 8. Stress distribution in the disc perpendicular to the load axis.

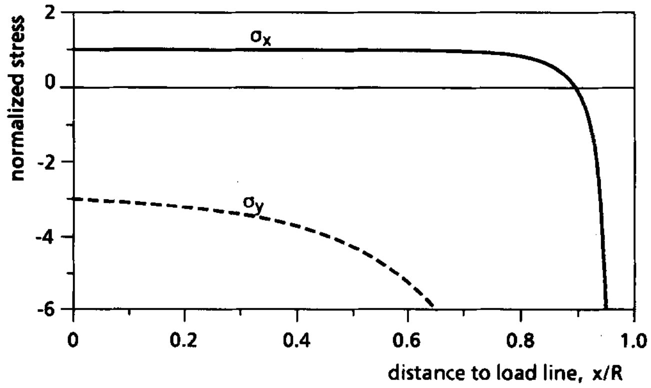

Fig. 9. Stress distribution in the disc along the load axis.

whereas the shear-insensitive criterion yields a distribution function which is compatible with the empirical distribution in terms of a Kolmogorov–Smirnov test. A similar result was obtained by comparing the Weibull distributions obtained with various test series.[9]

The agreement between theory and experiment appears to be slightly better for the silicon nitride materials than for the stoneware material, although in all cases the discrepancies between predicted and measured distributions are within the range of statistical uncertainty. However, this tendency may be attributed to the fact that for the silicon nitride materials the empirical distributions are based on fractographic evidence, whereas the results for the stoneware rely completely on the indications of the logical circuit. This may reduce the accuracy of the experimental values for the brittle fracture loci.

Conclusions

The cumulative distribution function of the fracture loci can be derived using the local risk of rupture. As the distribution function depends on the multiaxiality criterion in a way similar to the failure probability of the multiaxial Weibull theory, this quantity can be used to discriminate between various criteria. The advantage of this procedure is that only specimens of a specific type have to be compared with each other, and the well-known problems concerning different manufacturing routines and surface-finishing procedures are avoided, which may greatly influence the results obtained with test series performed with different kinds of specimens. The cumulative distribution function of fracture loci was measured using low- and high-strength ceramics. The test method selected was the Brazilian disc test, because the complicated stress state prevailing in the specimens leads to great differences in the predictions obtained with different multiaxiality criteria. The comparison between theory and experiment indicates that the failure behaviour of natural flaws in the materials tested should be described by a shear-insensitive criterion. This means that if a planar crack is assigned to each natural flaw, this crack fails through pure mode I fracture.

References

1. Batdorf, S. B. & Crose, J. G., A statistical theory for the fracture of brittle structures subjected to nonuniform polyaxial stress. *J. Appl. Mech.*, **41** (1974) 267–72.
2. Batdorf, S. B. & Heinisch, H. L., Weakest link theory reformulated for arbitrary fracture criterion. *J. Am. Ceram. Soc.*, **61** (1978) 355–8.
3. Evans, A. G., A general approach for the statistical analysis of multiaxial fracture. *J. Am. Ceram. Soc.*, **61** (1978) 302–8.
4. Matsuo, Y., A probabilistic analysis of the brittle fracture loci under bi-axial stress state. *Bull. JSME*, **24** (1981) 290–4.
5. Thiemeier, T., Brückner-Foit, A. & Kölker, H., Influence of the fracture criterion on the failure probability of ceramic components. *J. Am. Ceram Soc.*, **74** (1991) 48–52.
6. Lamon, J., Statistical approaches to failure for ceramic reliability assessment. *J. Am. Ceram. Soc.*, **71** (1988) 106–12.
7. DIN 51110, Parts 1–3, Prüfung von keramischen Hochleistungswerkstoffen, 1990.
8. Brückner-Foit, A., Berweiler, W., Hollstein, T., Mann, A., Munz, D. & Schirmer, K.-S., Mechanical characterization of engineering ceramics. Final Report, IEA Annex II, Subtask 5, University of Karlsruhe, September 1993.
9. Brückner-Foit, A., Fett, T., Munz, D. & Schirmer, K.-S., Discrimination of multiaxiality criteria with the Brazilian disk test. *J. Eur. Ceram. Soc.*, in press.
10. Matsuo, Y. & Kitakami, K., On the statistical theory of fracture location combined with competing risk theory. In *Fracture Mechanics of Ceramics, Vol. 7*, eds R. C. Bradt *et al.* Plenum Press, New York, 1986, pp. 223–35.
11. Brückner-Foit, A., Heger, A. & Munz, D., Effect of proof testing on the failure probability of multiaxially loaded ceramic components. In *Life Prediction Methodologies and Data for Ceramic Materials, ASTM STP 1201*, eds C. R. Brinkmann & S. F. Duffy. American Society for Testing and Materials, Philadelphia, 1994.
12. Hellen, T. K. & Blackburn, W. S., The calculation of stress intensity factors for combined tensile and shear loading. *Int. J. Fract.*, **11** (1975) 605–17.
13. Jaeger, J. C. & Hoskins, E. R., Rock failure under the confined Brazilian test. *J. Geophys. Res.*, **71** (1966) 2651–5.
14. Marion, R. H. & Johnstone, J. K., A parametric study of the diametral compression test for ceramics. *Am. Ceram. Soc. Bull.*, **56** (1977) 998–1002.
15. Bernauer, G., Untersuchung zu Anwendbarkeit des Spaltzugversuchs zur Ermittlung der Zugfestigkeit. Master Thesis, University of Freiburg, 1991.
16. Schäfer, R., Soltész, U. & Bernauer, G., 3-D-Finite-Elemente-Analyse zur Lokalisierung des Bruchursprungs im Spaltzugversuch, *IWM-Report W 3/95*, Fraunhofer-Institute for Mechanics of Materials, Freiburg, 1995.
17. Thoman, D. R., Bain, L. J. & Antle, C. E., Inferences of the parameters of the Weibull distribution. *Techometrics*, **11** (1969) 445–60.
18. Hondros, G., The evaluation of Poisson's ratio and the modulus of materials of a low tensile resistance by the Brazilian disk test with particular reference to concrete. *Australian J. Appl. Sci.*, **10** (1959) 243–68.